Sustainable Materials and Technologies 38 (2023) e00721

Contents lists available at ScienceDirect

Sustainable Materials and Technologies

journal homepage: www.elsevier.com/locate/susmat

Antimelanogenic potential of brewer's spent grain extract through modulation of the MAPK/MITF axis

Yu Jin Shon [a], Wook Chul Kim [b], Seung-Hong Lee [b], Sujung Hong [a], Seon-Young Kim [c], Mi Hee Park [c], Pomjoo Lee [d], Jihoon Lee [d], Kang Hoon Park [d], Wonchul Lim [e,**], Tae-Gyu Lim [a,e,*]

[a] Department of Food Science & Biotechnology, Sejong University, Seoul 05006, Republic of Korea
[b] Department of Medical Science, Soonchunhyang University, Asan 31538, Republic of Korea
[c] Jeonju AgroBio-Materials Institute, Jeonju-si, 54810, Republic of Korea
[d] RAFIQ Cosmetics Co.,Ltd., Republic of Korea
[e] Department of Food Science & Biotechnology, and Carbohydrate Bioproduct Research Center, Sejong University, Seoul 05006, Republic of Korea

ARTICLE INFO

Keywords:
Brewer's spent grain
By-product
Up-cycling
Melanin
MAPK

ABSTRACT

Beer brewing produces >39 million tons of brewer's spent grain (BSG) per year worldwide. Although BSG is rich in protein, fiber, and phytochemicals, it is mainly used as livestock feed, and some is discarded. In this study, we attempted to assess the antimelanogenesis effects of BSG and identify the functional components. To this end, we investigated the antioxidant and antimelanin synthesis effects of a BSG extract (BSGE). The results showed that BSGE has high DPPH radical-scavenging activity and inhibited α-MSH-induced melanin synthesis in B16F10 cells cultured in both 2D and 3D environments. BSGE also reduced the expression levels of MITF, TRP-1, TRP-2, and tyrosinase in B16F10 cells by regulating the MAPK pathway. We confirmed the skin-whitening effect of BSGE in 3D reconstituted human skin and zebrafish embryo models. HPLC analysis showed that BSGE contains ferulic acid and *p*-coumaric acid, which are known to have whitening effects. Thus, BSGE can be used in multifunctional cosmetics as a sustainable ingredient with antioxidant and skin-whitening properties.

1. Introduction

The amount of brewer's spent grain (BSG), the major residual by-product of beer brewing (85%), exceeds 39 million tons per year worldwide. In the European Union, approximately 3.4 million tons of BSG is generated each year [1]. BSG is currently considered an industrial waste, and it is used only as livestock feed. BSG contains approximately 20% protein, 70% fiber, and a high amount of phenolic compounds, mostly from barley grain husks; therefore, it has potential as a nutritional and functional ingredient [2]. BSG is particularly rich in hydroxycinnamic acids, including *p*-coumaric, ferulic, and caffeic acids, which have antioxidant, anti-inflammatory, anti-atherosclerotic, and anticancer effects [3–5]. Hydroxycinnamic acid (HCA) derivatives are well known cosmeceutical substances [6]. However, the inhibitory effects of BSG on melanogenesis have yet to be examined.

Melanin is a natural pigment present in most organisms that determines the color of skin and hair and provides protection against ultraviolet (UV) irradiation [7]. Melanocytes, located mainly in the epidermal layer and hair follicles of human skin, contain melanosomes, organelles that synthesize, store, and transport melanin [8,9]. Melanin synthesis is stimulated by various cytokines such as α-melanocyte stimulating hormone (α-MSH), stem cell factor (SCF), endothelin-1 (ET-1), and adrenocorticotropic hormone (ACTH) [10]. Tyrosinase, tyrosinase-related protein-1 (TRP-1), and tyrosinase-related protein-2 (TRP-2) are key enzymes in melanin synthesis [9]. During melanin synthesis, the substrate tyrosine is converted to a melanin polymer, which is a mixture of two pigments called eumelanin and pheomelanin, by tyrosinase, TRP-1, and TRP-2 [11]. Transcription of these melanin synthesis-related enzymes in melanocytes is regulated by microphthalmia-associated transcription factor (MITF) [12].

The mitogen-activated protein kinase (MAPK) pathway is an intracellular protein chain that transmits signals from receptors on the cell surface to the nucleus. MAPKs are grouped into three major families: extracellular signal-regulated kinases (ERKs), c-Jun N-terminal kinases (JNKs), and stress-activated protein kinases (p38/SAPKs). ERKs promote the ubiquitin-mediated proteasomal degradation of MITF under

* Corresponding author at: Department of Food Science & Biotechnology, Sejong University, Seoul 05006, Republic of Korea.
** Corresponding author.
E-mail addresses: wlim@sejong.ac.kr (W. Lim), tglim@sejong.ac.kr (T.-G. Lim).

https://doi.org/10.1016/j.susmat.2023.e00721
Received 9 May 2023; Received in revised form 8 September 2023; Accepted 21 September 2023
Available online 30 September 2023

phosphorylation conditions. JNK, which is involved in the proliferation and apoptosis of cancer cells, regulates melanogenesis by downregulating the expression of MITF [13,14]. In contrast, phosphorylation of p38 induced melanin production by upregulating MITF [15,16].

In this study, we investigated the antioxidant effect and antimelanogenic effects of brewer's spent grain extract (BSGE) on the murine melanoma cell line B16F10, a 3D human skin model, and a zebrafish embryo model. BSGE reduced melanin content and the expression levels of enzymes and a key transcription factor (MITF) associated with melanogenesis in B16F10 cells and 3D human skin and zebrafish embryo models. In addition, BSGE downregulated phosphorylation of p38 and upregulated phosphorylation of ERK1/2 and JNK in a time-dependent manner. Collectively, these results suggested that BSGE has potential for use as a sustainable ingredient in skin-whitening cosmetics.

2. Materials and methods

2.1. Reagents and antibodies

2,2-Diphenyl-1-picrylhydrazyl (DPPH) was purchased from Cayman Chemicals (Ann Arbor, MI, USA). The phenolic compound assay kit was obtained from Abcam (Cambridge, UK). The flavonoid compound assay kit was purchased from Cell BioLabs (St. Louis, MO, USA). 2,2′-Azino-bis (3-ethylbenzothiazoline-6-sulfonic acid) diammonium salt, potassium persulfate vitamin C, 3,4-dihydroxyphenylalanine (L-DOPA), mushroom tyrosinase, and α-MSH were obtained from Sigma-Aldrich (St. Louis, MO, USA). Hydrogen peroxide was purchased from Glentham Life Science Ltd. (Wiltshire, UK). Cell lysis buffer was purchased from Cell Signaling Technology (Danvers, MA, USA). The Pierce BCA Protein Assay Kit was purchased from Thermo Fisher Scientific (Waltham, MA, USA). Monoclonal or polyclonal antibodies against tyrosinase, TRP-1, TRP-2, p38, and JNK were obtained from Santa Cruz Biotechnology (Dallas, TX, USA). Antibodies against phospho-p38 and phospho-SAPK/JNK were purchased from Cell Signaling Technology. An antibody against phosho-ERK1/2 was acquired from R&D Systems (Minneapolis, MN, USA).

2.2. Preparation of brewer's spent grain extract

Brewer's spent grains (10 g) were extracted using water at 70 °C for 3 h. The extracted solution was then filtered through filter paper (Whatman, Buckinghamshire, UK). The obtained filtrate was freeze-dried. The yield of the BSGE was 6.68%, and it was stored at −70 °C until used in subsequent experiments.

2.3. DPPH radical scavenging activity assay

A DPPH solution (0.2 mM DPPH in 80% methanol) was prepared. Then, 80 μL of BSGE (6.25–800 μg/mL) was mixed with 80 μL of DPPH solution. After the mixture was shaken vigorously for 30 min in the dark, the absorbance was measured at 517 nm using a Cytation 1 microplate reader (BioTek, Winooski, VT, USA). DPPH radical scavenging activity (%) was calculated against the control (distilled water) after subtracting the DPPH untreated control.

2.4. ABTS radical scavenging activity

The ABTS assay described by previous study [17] was used to determine the ABTS assay. The ABTS radical cation ($ABTS^{\bullet+}$) was produced by reacting 7 mM ABTS stock solution and 2.45 mM potassium persulfate in equal quantities. Then, the mixture was left in the dark at room temperature for 16 h until the reaction was completed and the absorbance was stable. The radical cation formed if further diluted with distilled water to adjust the absorbance value to 0.700 (± 0.02) at 734 nm. A 10 μL of different concentrations (25–800 μg/mL) of BSGE was mixed with 190 μL of $ABTS^{\bullet+}$ solution and allowed to stand in the dark for 6 min at room temperature. The absorbance was determined at 734 nm. The ABTS radical scavenging activity was then calculated using the following equation:

$$ABTS^{\bullet+}\ \text{radical scavenging effect}\% = [(A_0 - A_1)/A_0] \times 100.$$

where A_0 was the absorbance of the control, and A_1 was the absorbance of the treated sample.

2.5. Total antioxidant capacity (TAC) assay

Total antioxidant capacity (TAC) was determined by using an antioxidant assay kit (MAK187, Sigma-Aldrich), that allows the concentration and the efficacy of antioxidant substances to be evaluated, by quantifying the reduction of Cu^{2+} to Cu^{+} in the presence of antioxidants. As a standard antioxidant, Trolox was used to generate a calibration curve following the manufacturer's instruction. Add 100 μL of Trolox or BSGE (25–800 μg/mL) into wells. After adding the Cu^{2+} working solution, the mixture was shaken for 90 min in the dark, the absorbance was measured at 570 nm. The concentration of antioxidant was calculated with Trolox equivalents.

2.6. Hydrogen peroxide radical scavenging activity

A solution of hydrogen peroxide (50 mM) was prepared in distilled water. 40 μL of different concentrations (25–800 μg/mL) of BSGE (or Vit. C as the control) were added to a hydrogen peroxide solution (60 μL). Then, the mixture was added to 100 μL of sodium phosphate buffer (50 mM) and incubated for 40 min at 30 °C. Next, 10 μL of DCFDA (10 μM) added to wells. After transferring 100 μL of the mixture to a black 96-well plate, the fluorescence of DCF was detected by fluorescence spectroscopy with excitation/emission at 485 nm /535 nm. The hydrogen peroxide percentage scavenging activity was then calculated using the following equation:H_2O_2 scavenging effect % = $[(A_0\text{-}A_1)/A_0] \times 100$.

where A_0 was the fluorescence of the control, and A_1 was the fluorescence of the treated sample.

2.7. Cell culture

Murine melanoma B16F10 cells were obtained from the Korean Cell Line Bank (Seoul, Republic of Korea), maintained in Dulbecco's Modified Eagles Medium (DMEM) (HyClone, GE Healthcare, Little Chalfont, UK), supplemented with 10% (*v*/v) fetal bovine serum (FBS) (GIBCO, Waltham, MA, USA), and 1% (v/v) penicillin–streptomycin (Gibco, Waltham, MA, USA) at 37 °C in a 5% CO_2 incubator.

2.8. Measurement of melanin content

Melanin content was determined as previously described [18]. Briefly, B16F10 cells were seeded at a density of 2.5×10^5 cells per 60 mm^2 dish. After overnight incubation, the cells were pretreated with BSGE (25–100 μg/mL) for 1 h. Then, 100 nM of α-MSH was added, and the cells were incubated for 72 h. The conditioned media containing extracelluar melanin was collected and centrifuged at 12,000 ×*g* for 10 min. Then, the supernatant was transferred to a 96-well plate and estimated based on the absorbance at 490 nm.

2.9. L-DOPA staining

L-DOPA staining was performed as described previously [19]. Briefly, B16F10 cells (2.5×10^5 cells/dish) were cultured in 60 mm^2 dishes. Then, the cells were lysed with 1× cell lysis buffer (20 mM Tris-HCl [pH 7.5], 150 mM NaCl, 1 mM Na_2EDTA, 1 mM EGTA, 1% Triton, 2.5 mM sodium pyrophosphate, 1 mM beta-glycerophosphate, 1 mM Na_3VO_4, and 1 μg/mL leupeptin) (Cell Signaling Technology), and total

protein was quantified using the Pierce BCA Protein Assay Kit. Quantified protein was mixed with buffer containing 0.1% sodium dodecyl sulfate (SDS) and β-mercaptoethanol without heating to prepare samples for gel electrophoresis. Equal protein (13 μg) was separated by electrophoresis on a 10% sodium dodecyl sulfate polyacrylamide gel based on molecular weight. After electrophoresis, the gels were soaked in 0.1 M sodium phosphate buffer (pH 6.9) for 30 min, twice, and then incubated at 37 °C in the same buffer containing 2 mM L-DOPA for 1 h. Finally, the intensity of L-DOPA staining was visualized using a chemiluminescence reader (LuminoGraph III Lite; ATTO, Tokyo, Japan).

2.10. Western blot analysis

B16F10 cells were lysed with 1× cell lysis buffer, and total protein was quantified using the Pierce BCA Protein Assay Kit. Equal protein was separated using 10% sodium dodecyl sulfate-polyacrylamide gel electrophoresis and then transferred to PVDF membranes. The membranes were blocked with bovine serum albumin solution for 1 h and then incubated with the indicated primary antibody at 4 °C overnight. After incubation with a horseradish peroxidase-conjugated secondary antibody for 40 min, the intensity of the antibody-bound protein bands was visualized using a chemiluminescence reader. Relative protein expression was calculated using ImageJ (NIH, Bethesda, MD, USA).

2.11. Reconstituted three-dimensional human skin model

The three-dimensional culture human skin model, Neoderm-ME (Tego Science, Seoul, Republic of Korea), consists of normal human epidermal keratinocytes and normal human epidermal melanocytes [20,21]. Neoderm-ME was transferred to a 12-well plate in maintenance medium (Tego Science) containing BSGE or arbutin and incubated at 37 °C in 5% CO_2 for 7 days. The medium was changed once every 2 days. On day 7, skin pigmentation was observed under a microscope. The skin samples were fixed in 4% formaldehyde overnight at room temperature, embedded in paraffin, and sectioned using a microtome to 4 μm thickness. The sections were deparaffinized and stained with Fontana-Masson's Staining Kit (Abcam, Cambridge, UK). Briefly, sections were reacted with an ammoniacal silver solution at 60 °C for 30 min. After rinsing the slides with distilled water, the slides were incubated in 0.2% gold chloride solution at room temperature for 30 s, and then incubation in 5% sodium thiosulfate solution for 1 min. To stain the nuclei, sections were incubated in nuclear fast red solution for 5 min and quickly dehydrated three times with fresh absolute alcohol. Sections were mounted using a mounting medium (Agilent, Santa Clara, CA, USA).

2.12. Quantitative real-time polymerase chain reaction

Total RNA was extracted from the reconstituted three-dimensional human skin tissues using TRIzol reagent (15,596,026; Thermo Fisher Scientific). Complementary DNA was synthesized using amfiRivert cDNA Synthesis Platinum Master Mix (R5600–200; GenDEPOT, Katy, TX, USA) in a total reaction volume of 20 μL for 39 cycles. Quantitative PCR was conducted using AccuPower 2× GreenStar qPCR Master Mix (K-6253; Bioneer, Daejeon, Korea) on a CFX96 Touch Real-Time PCR Detection System (Bio-Rad, Hercules, CA, USA). The primer sequences are listed in Table S1.

2.13. Zebrafish culture and treatment

Zebrafish were obtained from a commercial dealer (Sin-yong aquarium, Cheonan, Korea). Wild-type zebrafish, 60 week age, were kept in a 3 L acrylic tank at 28.5 °C under a 14/10 h light/dark cycle at a mating ratio of 2 males to 2 females. BSGE was dissolved in 0.4% (*v*/v) dimethyl sulfoxide (DMSO). Zebrafish embryos were exposed to 50 and 100 μg/mL BSGE and 100 μg/mL arbutin for 3 days. Control zebrafish embryos were exposed to 0.4% (v/v) DMSO.

2.14. Melanin content in zebrafish embryos

Embryos were sonicated in PRO-PREP Protein Extraction Solution (Intron, Seoul, Republic of Korea). After centrifugation, the obtained pellet was dissolved in 500 μL of 1 N NaOH at 60 °C for 30 min. The mixture was vortexed vigorously to solubilize the melanin in the sample. Then, the optical density of the supernatant was measured at 490 nm using a microplate reader (Synergy HTX Multimode Reader; BioTeK).

2.15. HPLC analysis of BSGE

High-performance liquid chromatography (HPLC) was performed to determine the phenolic acid composition according to previous study some modifications [22]. Briefly, BSGE was separated using an HPLC-ELSD (Agilent 1100 series, Agilent Technologies, Santa Clara, CA, USA). Column separation was performed on an Agilent HC-C18(2) (4.6 × 250 mm, 5 μm). The injection volume was 10 μL, the flow rate was 0.3 mL/min, the column temperature was 25 °C, the mobile phase consisted of 0.1% formic acid in water (A) and 0.1% formic acid in acetonitrile (B), and the detection wavelength was 320 nm. The gradient program was as follows: 10% B before initiation, 10%–70% B for 70 min, and 10% B for 10 min, and was started 10 min before injection.

2.16. LC-high resolution mass spectrometry and experimental conditions

The identification and quantification of polyphenols in BSGE were achieved by a High-performance Liquid Chromatography-High Resolution MS/MS system with Orbitrap Exploris 120 mass spectrometer (Thermo Scientific, Hemel Hempstead, UK) according to previous study [23]. with some modifications. Chromatographic separation was accomplished with a ACQUITY UPLC BEH C18 Column, 130 Å, 1.7 μm, 1 mm × 100 mm (Waters Corp., Milford, MA. US). The injection volume was 5 μL, the flow rate was 0.4 mL/min, the column temperature was 40 °C, the mobile phase consisted of 0.1% acetic acid in water (A) and 0.1% acetic acid in acetonitrile (B), and the detection wavelength was 210 nm. The gradient program was as follows: 0 min, 2% B; 0–2 min, 8% B; 2–12 min, 20% B; 12–13 min, 30% B; 13–14 min, 100% B; 14–17 min, 100% B; 17–18 min, 2% B and the column was equilibrated for 7 min to initial conditions. Mass spectra were acquired in profile mode with a setting of 120,000 resolution at *m/z* 100–1500. Operation parameters were as follows: source voltage, 4 kV; sheath gas, 50 (arbitrary units); auxiliary gas, 10 (arbitrary units); sweep gas, 2 (arbitrary units); the ion transfer tube temperature, 325 °C, and the vaporizer temperature, 350 °C. BSGE was analyzed in full scan mode at a resolving power of 120,000 at *m/z* 100–1500 and data-dependent MS/MS events were acquired at a resolving power of 15,000. An isolation window (*m/z*) of 2 was used and precursors were fragmented by Higher-energy C-trap dissociation (HCD) with normalized collision energy of 15, 30, 60 (%). The identification of the volatile components was conducted based on the *p*-coumaric acid and ferulic acid standards at concentration 10 μg/mL.

2.17. Statistical analysis

All statistical analyses were performed using SPSS software (version 20.0; SPSS, Chicago, IL, USA). Data are mean ± standard deviation (SD). Statistical significance was determined using Student's *t*-test for single statistical comparisons, and p values <0.05 were regarded as significant.

3. Results

3.1. Antioxidative activity, total polyphenol & flavonoid contents, and tyrosinase activity of BGSE in α-MSH-stimulated B16F10 cells

A DPPH free radical scavenging activity assay, ABTS radical scavenging activity assay, Total antioxidant capacity (TAC) assay, and

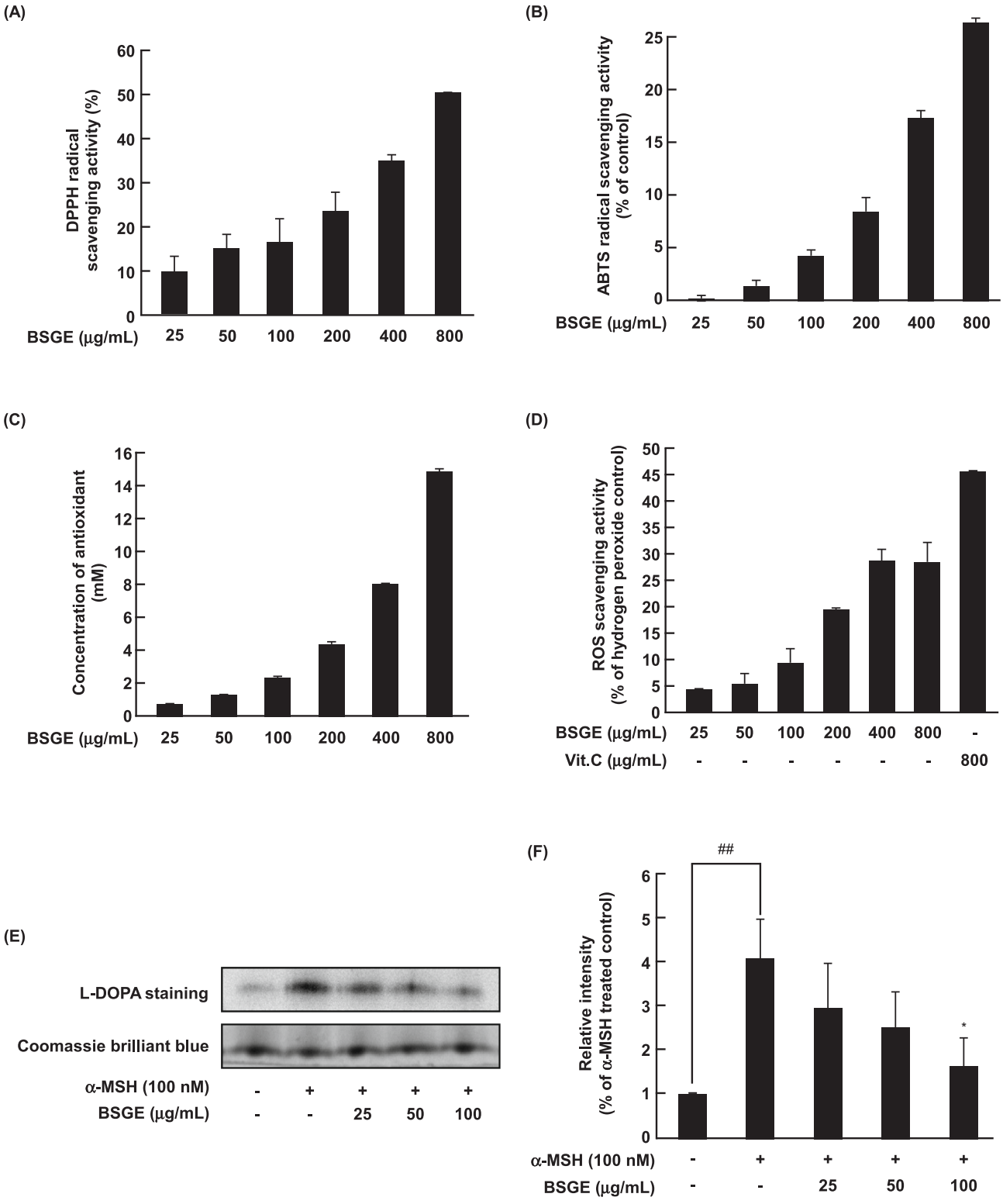

Fig. 1. Effect of BSGE on DPPH free radical scavenging and cellular tyrosinase activity. (A) Various concentrations of BSGE were used in a DPPH assay. (B) Various concentration of BSGE were used in a ABTS assay. (C) Various concentration of BSGE were used in a total antioxidant capacity assay. (D) Various concentration of BSGE and Vit.C (800 μg/mL) were used in a hydrogen peroxide scavenging assay. (E) The effect of BSGE on cellular tyrosinase activity in α-MSH-induced B16F10 cells was estimated using L-DOPA staining. (F) Results are expressed as percentages of the untreated control. Representative data (mean ± SD) from three independent experiments are shown. $^{*}p < 0.05$, $^{**}p < 0.01$, $^{***}p < 0.001$ vs. the untreated control.

Table 1
Total polyphenol and total flavonoid contents of BSGE.

	Total polyphenol contents (mM CA equivalents)	Total flavonoid contents (μg QE/mg)
BSGE	0.11 ± 0.00	1.55 ± 0.05

Hydrogen peroxide radical scavenging activity were performed to investigate the antioxidant activity of BSGE. The radical scavenging activity of BSGE was evaluated at concentrations of 25 to 800 μg/mL, and the radical scavenging activity of the control (distilled water) was set to 0. The DPPH free radical and ABTS cation radical scavenging activity of BSGE increased in a dose-dependent manner (Fig. 1A, B). At the same concentration, BSGE had a dose-dependently antioxidant property (Fig. 1C). Also, there was progressive enhancement in hydrogen peroxide radical scavenging on increasing the concentration of BSGE (Fig. 1D). Next, we analyzed the total polyphenol and flavonoid contents of BSGE using total polyphenol content and total flavonoid content assays. The assays detected 0.11 ± 0.00 mM catechin equivalents and 1.55 ± 0.05 μg QE/mg, respectively, in the BSGE (Table 1).

Tyrosinase is an enzyme used to evaluate the whitening activity effect and catalyzes the rate-determining step of melanin biosynthesis

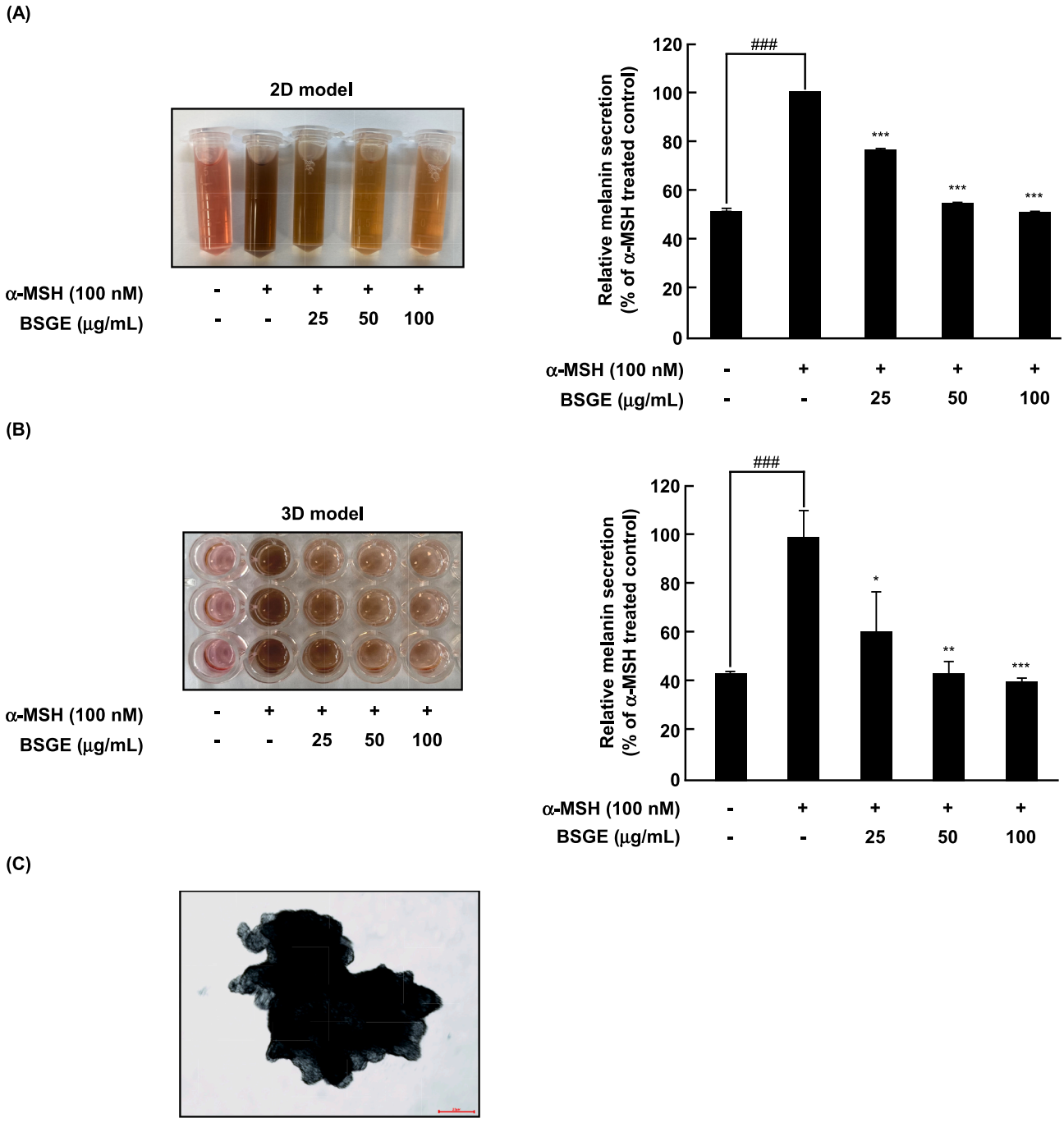

Fig. 2. BSGE reduces melanin secretion from B16F10 cells stimulated with α-MSH. (A) The effect of BSGE on extracellular melanin contents in a 2D culture of B16F10 cells stimulated with α-MSH. (B) The effect of BSGE on extracellular melanin contents in a culture of α-MSH-induced B16F10 cells in a ULA round-bottom plate. (C) Morphology of B16F10 cells grown in a ULA round-bottom plate. Results are expressed as percentages of the untreated control. Representative data (mean ± SD) from three independent experiments are shown. *$p < 0.05$, **$p < 0.01$, ***$p < 0.001$ vs. the untreated control.

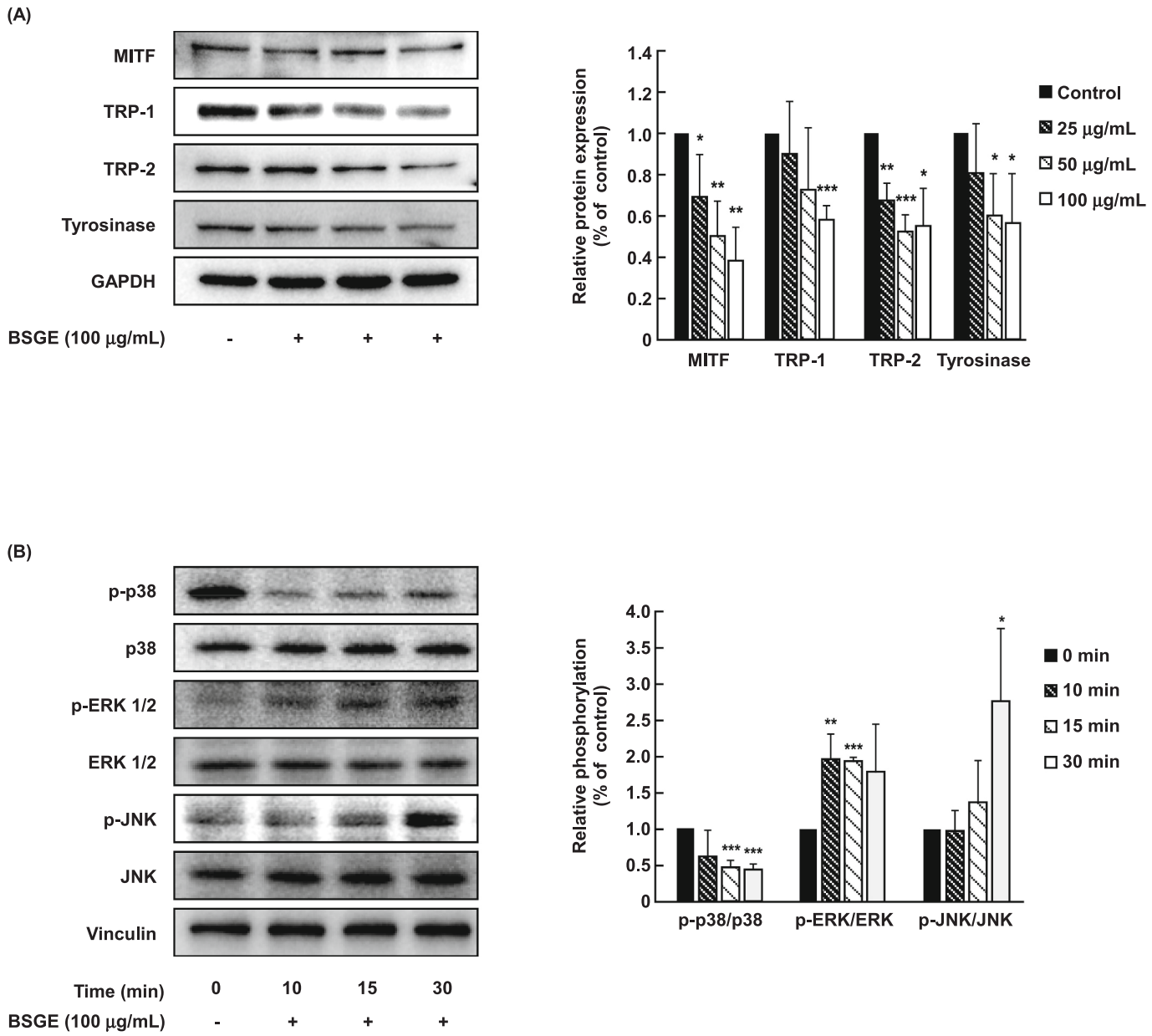

Fig. 3. BSGE reduces the expression of melanogenesis-related proteins in B16F10 cells by regulating the MAPK pathway. (A) Effects of BSGE on the protein expression of MITF, TRP-1, TRP-2, and tyrosinase in B16F10 cells were assessed using western blotting analysis. (B) Effects of BSGE on activation of the MAPK signaling pathway in B16F10 cells. Phosphorylation of MAPKs was assessed using western blotting analysis. Target protein expression was normalized to vinculin expression, and protein phosphorylation was normalized to non-phosphorylated protein levels. MAPKs, mitogen-activated protein kinase; Results are expressed as percentages of the untreated control. Representative data (mean ± SD) from three independent experiments are shown. *$p < 0.05$, **$p < 0.01$, ***$p < 0.001$ vs. the untreated control.

[24]. To confirm the inhibitory effect of the BSGE against intracellular tyrosinase activity of B16F10 cells, L-DOPA staining was performed. B16F10 cells were treated with 25, 50, and 100 μg/mL of BSGE. As result, stained L-DOPA was dose-dependently decreased by exposure to BSGE (Fig. 1E, F). These results suggested that BSGE has inhibitory effects on melanin synthesis through suppressing intracellular tyrosinase activity.

3.2. *Inhibitory effect of BSGE on melanin secretion by B16F10 cells grown on a two-dimensional surface and in a three-dimensional culture environment*

Melanin synthesized in melanocytes is packaged and transferred to neighboring keratinocytes in the skin epidermis. Melanocytes cultured in a 3D environment are more similar to skin than melanocytes cultured in a 2D environment. In particular, melanocytes can better synthesize melanin in a 3D environment [25]. To confirm the antimelanogenic effect of the BSGE, we measured the extracellular melanin contents in cultures of B16F10 cells (grown in 60 mm^2 dishes) treated with different concentrations of BSGE (25, 50, and 100 μg/mL). Melanin content was reduced by BSGE in a dose-dependent manner (Fig. 2A). Melanin content was also decreased by BSGE in a dose-dependent manner in 3D cell cultures (Fig. 2B). Cells cultured in the 3D environment were spheroid in shape (Fig. 2C).

3.3. *Effect of BSGE on melanogenesis-related signaling pathway*

To determine whether BSGE affect the expression of the

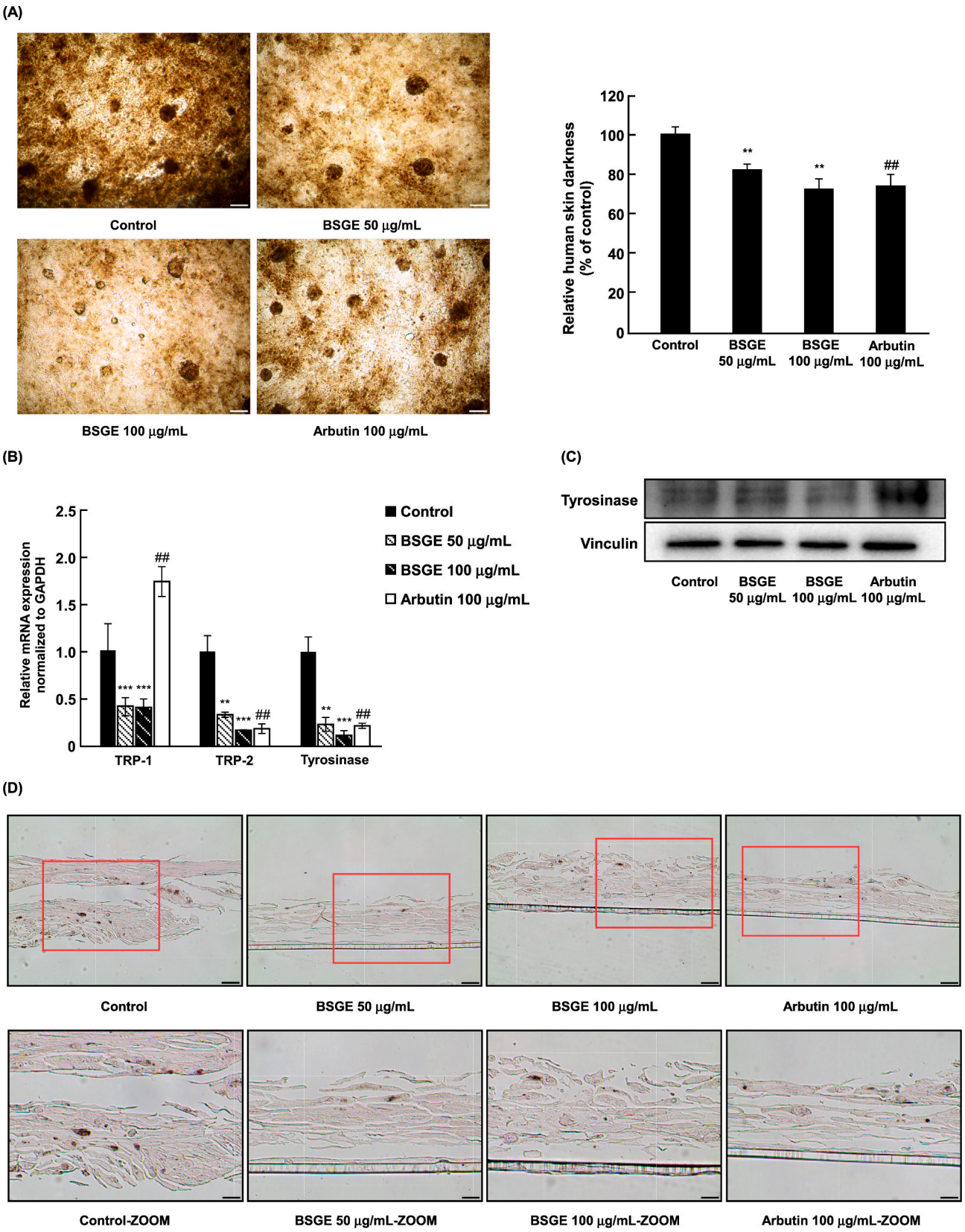

Fig. 4. BSGE has an antimelanogenic effect in a skin-equivalent Neoderm-ME model. The upper stratum corneum of a human skin model was treated with 50 and 100 μg/mL of BSGE or 100 μg/mL of arbutin every other day for 7 days. (A) Effects of BSGE on melanin synthesis and skin darkness in a 3D human skin model. Scale bar = 100 μm. Data are mean ± SD ($n = 3$). (B) Effect of BSGE on the mRNA expression of TRP-1, TRP-2, and tyrosinase in a 3D human skin model was measured using quantitative real-time PCR. Data are mean ± SD (n = 3). *p < 0.05, **p < 0.01, ***p < 0.001 vs. the untreated control. (C) Effect of BSGE on tyrosinase expression in a 3D human skin model was analyzed using western blotting. (D) Melanin pigmentation of a 3D human skin model was observed using Fontana-Masson staining. Scale bar = 100 μm.

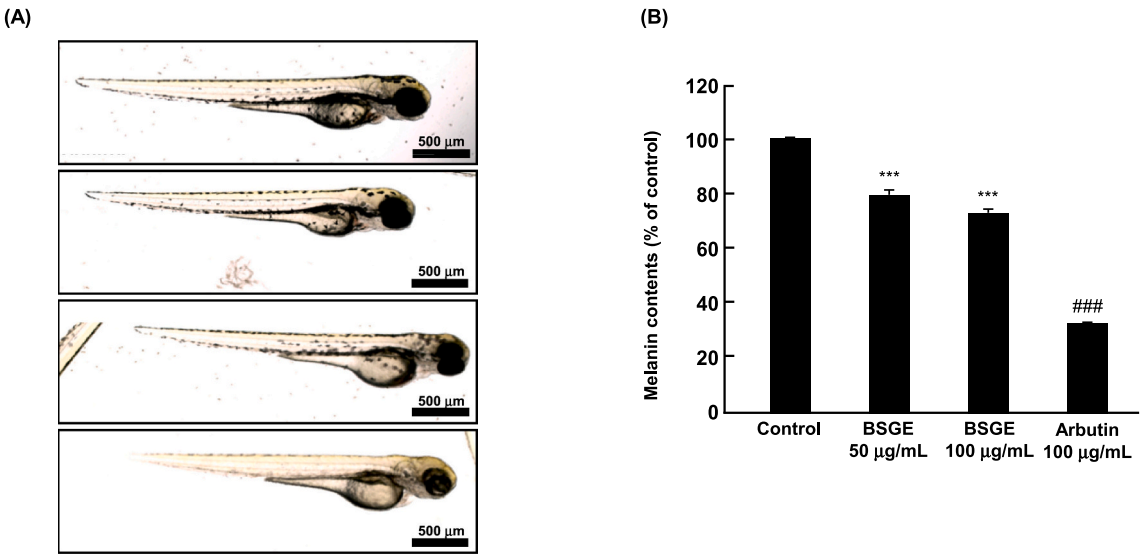

Fig. 5. BSGE inhibits melanin synthesis in a zebrafish embryo model. (A) Effects of BSGE on the melanin accumulation in zebrafish. (10 × 4 magnification) The images were taken with a 4×/0.13. Scale bar = 500 μm. (B) BSGE reduced melanin contents in zebrafish embryos. Fifteen embryos were pooled for each assay. Data are mean ± SD (n = 3). *p < 0.05, **p < 0.01, ***p < 0.001 vs. the untreated control.

melanogenesis-related proteins MITF, TRP-1, TRP-2, and tyrosinase, their protein levels were examined using western blot analysis in B16F10 cells after treatment with different concentrations of BSGE (25, 50, and 100 μg/mL), which are concentrations that did not affect survival (Fig. S1). The expression levels of MITF, TRP-1, TRP-2, and tyrosinase in B16F10 cells were decreased after treatment with BSGE in a dose-dependent manner (Fig. 3A). These results indicated that the antimelanogenesis effect of BSGE was related to downregulation of MITF and other melanogenesis-related proteins.

MITF is regulated by various signaling pathways, including mitogen-activated protein kinase (MAPK) pathways [15]. To examine the possible role of the MAPK pathway in the modulation of melanogenesis, we examined the phosphorylated and total protein levels of the important MAPK pathway members p38, ERK, and JNK in B16F10 cells treated with BSGE (100 μg/mL) over time. The levels of phosphorylated p38 decreased in a time-dependent manner, whereas the levels of phosphorylated ERK and JNK increased (Fig. 3B). These results suggested that BSGE regulates MITF proteins via the MAPK signaling pathway.

3.4. Inhibitory effect of BSGE on melanin synthesis in a 3D human skin model

To confirm the inhibitory effect of BSGE on melanogenesis in a 3D human skin model, we treated reconstituted 3D human skin with 50 and 100 μg/mL BSGE and used arbutin as a positive control. After 7 days of treatment, we observed that BSGE treatment reduced the darkness of the model epidermis in a dose-dependent manner (Fig. 4A). We then examined the mRNA and protein levels of TRP-1, TRP-2, and tyrosinase in the samples. BSGE treatment significantly decreased the mRNA levels of TRP-1, TRP-2, and tyrosinase (Fig. 4B). Tyrosinase protein levels were also significantly decreased following BSGE treatment (Fig. 4C). Consistently, Fontana-Masson staining showed that melanin levels in the epidermis were decreased by BSGE treatment (Fig. 4D). These results suggest that BSGE suppresses melanogenesis in 3D human skin by regulating melanin synthesis-related genes and proteins.

3.5. Inhibitory effect of BSGE on melanin synthesis in zebrafish embryos

The zebrafish embryo model has been widely used as an alternative to rodent models [26]. To evaluate the in vivo whitening effect of BSGE, zebrafish embryos were exposed to 50 and 100 μg/mL of BSGE for 3 days. At the end of the experiment, BSGE did not affect the survival and hatching rates at doses of 50 and 100 μg/mL (Fig. S2). Arbutin, a well-known tyrosinase inhibitor, was used as a positive control [27]. BSGE treatment reduced the intensity of melanin pigment in the zebrafish embryos in a dose-dependent manner (Fig. 5A). We also assessed the melanin content in the zebrafish embryos and found that the melanin content was also decreased in a dose-dependent manner (Fig. 5B).

3.6. HPLC and LC-MS/MS analysis of phenolic compounds of BSGE

To identify the components of BSGE responsible for inhibiting melanin synthesis, HPLC analysis was performed to detect caffeic acid, ferulic acid, and *p*-coumaric acid, which are the major phenolic acids in BSG. BSGE and phenolic acid standards were analyzed, and a representative chromatogram was obtained at a wavelength of 320 nm (Fig. 6). The most dominant phenolic acids in the BSGE were ferulic acid (peak b) and *p*-coumaric acid (peak c), whereas no peak for caffeic acid was observed. The total specific phenolic acid content in the BSGE is shown in Table 2. Our results were consistent with those of previous studies which showed that the major phenolic acids in BSG were ferulic acid and *p*-coumaric acid [28]. Furthermore, we used the Orbitrap Exploris 120 mass spectrometer to further identify ferulic acid and *p*-coumaric acid in BSGE. A standard mixture chromatogram of phenolic acids by LC-MS/MS is presented in Fig. S3. A diluted BSGE chromatogram is also given in Fig. 6B. According to the LC-MS/MS experiment, ferulic acid and *p*-coumaric acid were found in BSGE: *p*-coumaric acid (*m/z* 163.0402), ferulic acid (*m/z* 193.0507) (Fig. 6C and D). Moreover, *p*-coumaric acid and ferulic acid were confirmed by comparing the retention time and the MS^2 spectrum with pure standards (Fig. 6C, D, and S3).

4. Discussion

Studies on the utilization of food wastes and by-products, such as peels, pomace, and seeds, have recently increased. These food manufacturing wastes and by-products contain numerous valuable compounds, such as starches, proteins, and bioactive substances, which can provide opportunities for the food packaging industry [29]. Moving toward a zero-waste operation that reduces agricultural industrial waste through utilization of new, high-added value products can reduce the costs of waste disposal and minimize environmental pollution [30].

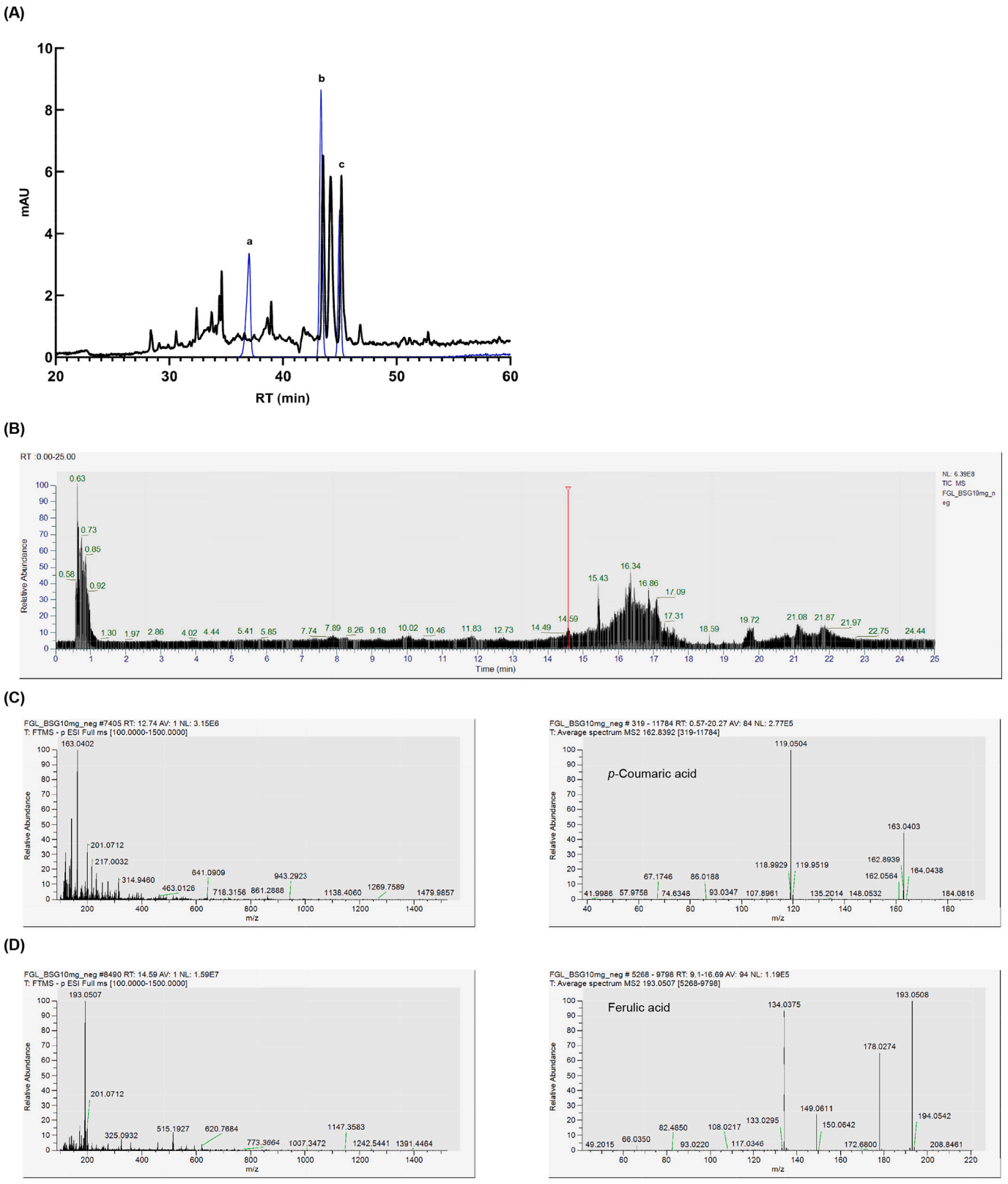

Fig. 6. Chromatogram of the active compounds in BSGE as determined using HPLC-UV and LC-MS/MS analysis. (A) HPLC chromatogram of BSGE at 320 nm, the three peaks (blue) correspond to the three standards expected to be present in BSGE: caffeic acid (a), ferulic acid (b), and *p*-coumaric acid (c). The main peaks (black) in BSGE were identified as ferulic acid, an unknown compound, and *p*-coumaric acid. (B) Chromatogram of untargeted UPLC-HRMS from BSGE. (C) LC-MS/MS spectrum of *p*-coumaric acid in BSGE. (D) LC-MS/MS spectrum of ferulic acid in BSGE.

Table 2
Chemical composition analysis of phenolic acids of water extract from BSG by HPLC.

Compound	Retention time (minutes)	Concentration (μg/g)
Ferulic acid	43.541	76
p-Coumaric acid	45.143	116

Approximately 3.4 million tons of BSG is produced annually in the European Union [31]. BSG is the insoluble solid fraction from the wort filtration step to be fermented into beer during brewing, which includes malting, milling, crushing, rooting, boiling, wort cooling, and fermentation. BSG consists of the seed coat, husk, and pericarp layer covering the barley grain. It is composed of approximately 70% lignocellulosic fiber, 20% protein, and 10% lipid and also contains vitamins, minerals, amino acids, and phenolic compounds. Correspondingly, we confirmed 194.55 μg/mg of protein, 0.11 ± 0.00 mM catechin equivalents, and 1.55 ± 0.05 μg QE/mg, respectively, in the BSGE (Table 1). Despite the sustainable high-volume production and low cost of BSG, currently, there are no economically viable applications [29]. Approximately 20 kg of wet BSG is obtained per 100 L of beer, indicating the sustainable supply of this raw material. Most of the BSG produced (70%) is used for livestock feed, 10% is used for biogas production, and the remaining 20% goes to landfills. In terms of the environmental impact, BSG poses a high risk, as approximately 514 kg of CO_2 greenhouse gas can be released per ton if it discarded without pretreatment [32]. Various possibilities for the utilization of BSG have been proposed, including using it as a material for bakery products [33]. However, research on its antimelanogenic effects is lacking. This study focused on the antimelanogenic effects of BSG and its mechanism of action in B16F10 cells and 3D human skin and zebrafish embryo models.

In the skin, melanin production is induced by various signal stimuli, including α-MSH, and it protects the epidermis from harmful factors, such as UV rays and oxidative stress [8]. However, excessive melanin production can cause spots, freckles, and skin cancer. Therefore, numerous studies have been conducted to develop natural or synthetic melanogenesis inhibitors [34]. However, one developed synthetic compound, YT16i, was highly toxic and caused major morphological abnormalities and altered cardiac function in zebrafish embryos [35]. Although natural product-derived melanogenesis inhibitors, such as kojic acid and arbutin, have been discovered, there are no reports on the development of melanogenesis inhibitors from by-products.

The antioxidant activity of a natural product is typically measured based on its ability to scavenge DPPH free radicals, ABTS cation radicals, and hydrogen peroxide [36]. Furthermore, phytochemicals, including phenolic compounds, carotenoids, vitamins, volatiles, and organic acids, are thought to improve health due to their antioxidant, anti-inflammatory, antibacterial, and anticancer activities. It is reported that melanogenesis produces hydrogen peroxide (H_2O_2) and reactive oxygen species (ROS), which lead to the generation of high-grade oxidative stress in melanocytes [37]. In this study, BSGE showed DPPH, ABTS radical, and hydrogen peroxide scavenging activity (Fig. 1A–C), and the total antioxidant capacity increased in a dose-dependent manner (Fig. 1D). Therefore, the anti-oxidative capacity of BSGE, based on the results, is expected to lead to improved anti-melanogenic effect.

Tyrosinase is an important rate-limiting enzyme in melanogenesis. Tyrosinase converts DOPA to DOPA quinone, leading to melanin polymerization [11]. To evaluate the in vitro antimelanogenic effects of BSGE, we employed the murine melanoma B16F10 cell line, which is widely used to evaluate skin whitening effects. In this study, melanin synthesis was induced with α-MSH, which is the most commonly used inducer to assess antimelanogenesis effects [38]. BSGE significantly suppressed intracellular tyrosinase activity in B16F10 cells (Fig. 1B). In addition, extracellular melanin content in a 2D culture of B16F10 cells was reduced by BSGE in a dose-dependent manner (Fig. 2A). Although 2D cell culture platforms are the most commonly used, they differ from the real in vivo environment, as cells in 2D environments tend to respond differently to external stimuli, such as drugs, from cells cultured in 3D environments [25]. Interestingly, BSGE also significantly reduced α-MSH-induced melanogenesis in B16F10 cells cultured in a 3D environment (Fig. 2B). The decreases in the protein levels of the melanogenesis-related enzymes TRP-1, TRP-2, and tyrosinase in B16F10 cells were consistent with the antimelanogenic effect of BSGE (Fig. 3A).

MITF is a major transcription factor that regulates the expression of TRP-1, TRP-2, and tyrosinase [12]. Previous studies have shown that MITF is regulated through multiple pathways, including the MAPK pathway [39]. We found that BSGE significantly reduced MITF expression (Fig. 3A). To understand the mechanism underlying the inhibitory action of BSGE on MITF expression, we examined its effect on the activation of the MAPK pathway, a regulatory signaling pathway upstream of MITF. Three MAPKs were evaluated, and the result showed that phosphorylation of p38 was significant downregulated, while phosphorylation levels of ERK and JNK were upregulated by BSGE treatment (Fig. 3B). Several studies have reported that p38 acts as a positive regulator of MITF, whereas ERK and JNK act as negative regulators of MITF [15]. Our findings suggest that BSGE increases the phosphorylation of ERK and JNK while decreasing the phosphorylation of p38, thereby inhibiting the expression of melanogenesis-related enzymes, leading to the inhibition and degradation of MITF. As mentioned in the manuscript, the focus of our study is on the multi-functionality of BSGE, as it not only inhibited the effect of melanin production but also confirmed its antioxidant effect. To determine whether the anti-melanogenesis effect of BSGE is due to the antioxidant effect or vice versa, further study is required. According to a previous study, hydrogen peroxide has a role as an inducer of elevated tyrosinase level in melanoma cells [40]. Some studies have shown that antioxidants have anti-melanogenic activity through scavenging ROS and interacting with melanogenic intermediates [41]. Therefore, antioxidant could act as an antimelanogenic agent by scavenging ROS, and we could hypothesize that BSGE has the potential to inhibit the tyrosinase level due to its free radical scavenging activity. In contrast, previous research showed that an increase in ROS promotes the phosphorylation of ERK, leading to MITF degradation [42,43]. This opposite role of ROS on melanogenesis may be that ROS primarily functions as a secondary signal messenger in the body at normal levels, but they can have detrimental effects on cells at excessive levels [44]. Therefore, it is believed that further research is needed to study the role of free radicals in the inhibition of melanin production by BSGE.

The 3D pigment human skin model is an experimental model that reproduces the morphology and physiology of human skin better than cell lines or animal models [45]. Recently, 3D reconstituted human skin models have been used to screen various pharmaceuticals and cosmetics. The level of melanin produced in the BSGE-treated model was similar to that induced by arbutin (Fig. 4A), a competitive tyrosinase inhibitor [46]. BSGE treatment decreased the mRNA and protein levels of TRP 1 and 2 and tyrosinase (Fig. 4B and C). Based on these findings, it is possible to indirectly predict the whitening effect of BSGE on human skin.

Zebrafish, like other vertebrates, have pigment cells that arise from two embryogenesis [47]. Therefore, the zebrafish embryo model has been used in numerous studies to confirm the antimelanogenic effect of various compounds [48,49]. In fact, there are limitations in identifying tyrosinase, TRP-1, 2, MITF, and MAPKs using the zebrafish embryo model. Instead, we identified that BSGE significantly reduced melanin accumulation without negatively affecting zebrafish survival (Fig. 5A and 5 B). Although the survive rate in group treated with 100 μg/mL of BSGE showed 90% than that of control group, there is no problem according to ISO 10993 of Good Laboratory Practice designated by the U.S. Food and Drug Administration, which sets a standard of over 70% survival rate. Therefore, these results suggested that BSGE administration reduces melanin production without toxicity in zebrafish model.

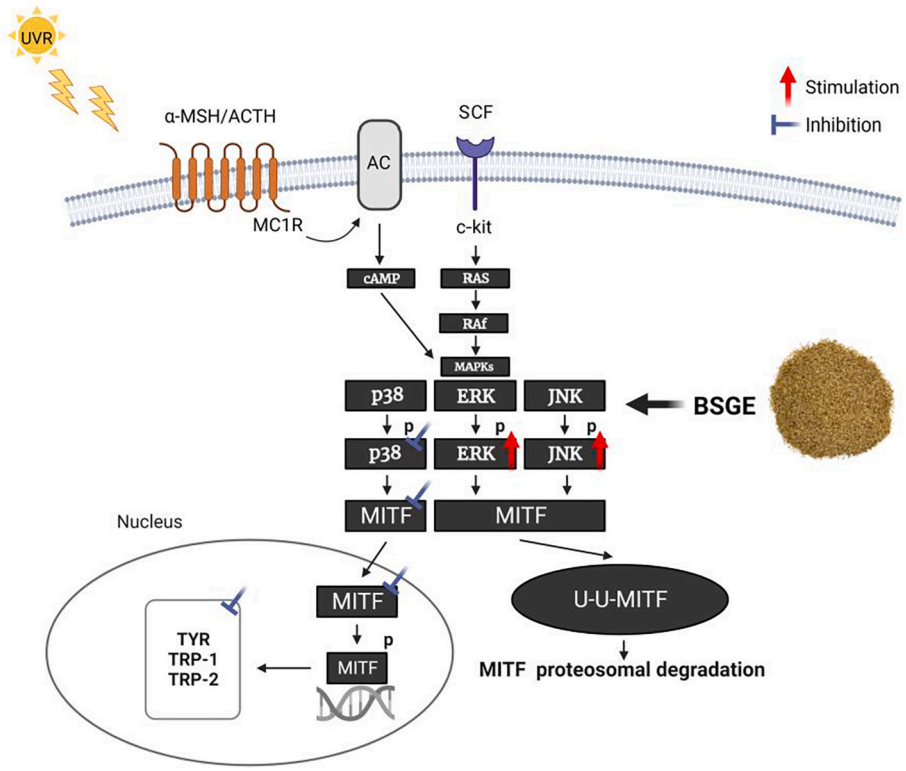

Fig. 7. Schematic diagram of the antimelanogenesis mechanism of BSGE, which involves regulation of the MAPK-MITF signaling pathway.

Therefore, unlike other synthetic compounds, the by-product-derived BSGE shows potential as a sustainable inhibitor of melanogenesis without toxic side effects.

To identify the key functional ingredients that confer the sustainable antimelanogenic effects of BSGE, HPLC-UV, and LC-MS/MS analyses were performed. We have identified ferulic acid and *p*-coumaric acid in BSGE. (Fig. 6). Interestingly, previous studies have reported that ferulic acid and *p*-coumaric acid have antimelanogenesis effects [6,50]. Based on this, we speculated that the ferulic acid and *p*-coumaric acid content of BSGE are key to its melanogenesis-inhibiting effect. In future studies, it will be necessary to determine how BSG-derived bioactive compounds, including ferulic acid and *p*-coumaric acid, affect the MAPK signaling pathway.

5. Conclusion

In summary, we confirmed the significant antimelanin synthesis effects of BSGE in melanoma cells cultured in 2D and 3D environments and in 3D reconstituted human skin and zebrafish embryo models. BSGE inhibited melanogenesis by suppressing the expression of melanogenesis-related genes or proteins via regulation of the MAPK pathway (Fig. 7). Therefore, BSGE is a potential whitening agent.

CRediT authorship contribution statement

Yu Jin Shon: Conceptualization, Data curation, Methodology, Formal analysis, Writing – original draft. **Wook Chul Kim:** Data curation, Formal analysis. **Seung-Hong Lee:** Data curation, Formal analysis. **Seon-Young Kim:** Writing – review & editing. **Mi Hee Park:** Writing – review & editing. **Pomjoo Lee:** Funding acquisition, Formal analysis. **Jihoon Lee:** Funding acquisition, Formal analysis. **Kang Hoon Park:** Funding acquisition, Formal analysis. **Wonchul Lim:** Methodology, Writing – review & editing. **Tae-Gyu Lim:** Project administration, Funding acquisition, Conceptualization.

Declaration of Competing Interest

The authors declare that they have no known competing financial interests or personal relationships that could have appeared to influence the work reported in this paper.

Data availability

No data was used for the research described in the article.

Acknowledgements

This work was supported by the Starting growth Technological R&D Program of MSS [S3201145] funded by the Ministry of SMEs and Startups (MSS, Korea), Bio & Medical Technology Development Program of the National Research Foundation (NRF) funded by the Ministry of Science & ICT(NRF-2022M3A9I5082349), National Research Foundation of Korea (NRF) grant funded by the Korea government (MSIT) (No. 2020R1C1C1004670), Basic Science Research Program through the National Research Foundation of Korea (NRF) funded by the Ministry of Education (2022R1A6A1A03055869), and Korea Basic Science Institute (National Research Facilities and Equipment Center) grant funded by the Ministry of Education (2023R1A6C101A045).

Appendix A. Supplementary data

Supplementary data to this article can be found online at https://doi.org/10.1016/j.susmat.2023.e00721.

References

[1] S.I. Mussatto, Brewer's spent grain: a valuable feedstock for industrial applications, J. Sci. Food Agric. 94 (7) (2014) 1264–1275.
[2] S.I. Mussatto, G. Dragone, I.C. Roberto, Brewers' spent grain: generation, characteristics and potential applications, J. Cereal Sci. 43 (1) (2006) 1–14.

[3] A.L. McCarthy, et al., The hydroxycinnamic acid content of barley and brewers' spent grain (BSG) and the potential to incorporate phenolic extracts of BSG as antioxidants into fruit beverages, Food Chem. 141 (3) (2013) 2567–2574.
[4] A.L. McCarthy, et al., In vitro antioxidant and anti-inflammatory effects of brewers' spent grain protein rich isolate and its associated hydrolysates, Food Res. Int. 50 (1) (2013) 205–212.
[5] C.S. Yang, et al., Inhibition of carcinogenesis by dietary polyphenolic compounds, Annu. Rev. Nutr. 21 (2001) 381–406.
[6] O. Taofiq, et al., Hydroxycinnamic acids and their derivatives: cosmeceutical significance, challenges and future perspectives, a review, Molecules 22 (2) (2017).
[7] M. Brenner, V.J. Hearing, The protective role of melanin against UV damage in human skin, Photochem. Photobiol. 84 (3) (2008) 539–549.
[8] A. Slominski, et al., Melanin pigmentation in mammalian skin and its hormonal regulation, Physiol. Rev. 84 (4) (2004) 1155–1228.
[9] J. Bonaventure, M.J. Domingues, L. Larue, Cellular and molecular mechanisms controlling the migration of melanocytes and melanoma cells, Pigment Cell Melanoma Res. 26 (3) (2013) 316–325.
[10] Y. Hushcha, et al., microRNAs in the regulation of melanogenesis, Int. J. Mol. Sci. 22 (11) (2021).
[11] J.H. Hwang, B.M. Lee, Inhibitory effects of plant extracts on tyrosinase, L-DOPA oxidation, and melanin synthesis, J. Toxicol. Environ. Health A 70 (5) (2007) 393–407.
[12] N. Arora, E.M. Siddiqui, S. Mehan, Involvement of adenylate cyclase/cAMP/CREB and SOX9/MITF in melanogenesis to prevent vitiligo, Mol. Cell. Biochem. 476 (3) (2021) 1401–1409.
[13] M. Wu, et al., C-kit triggers dual phosphorylations, which couple activation and degradation of the essential melanocyte factor Mi, Genes Dev. 14 (3) (2000) 301–312.
[14] D.S. Kim, et al., Sphingosine-1-phosphate decreases melanin synthesis via sustained ERK activation and subsequent MITF degradation, J. Cell Sci. 116 (Pt 9) (2003) 1699–1706.
[15] H. Choi, et al., Decursin prevents melanogenesis by suppressing MITF expression through the regulation of PKA/CREB, MAPKs, and PI3K/Akt/GSK-3beta cascades, Biomed. Pharmacother. 147 (2022) 112651.
[16] J.H. Kim, et al., JNK suppresses melanogenesis by interfering with CREB-regulated transcription coactivator 3-dependent MITF expression, Theranostics 10 (9) (2020) 4017–4029.
[17] N. Pellegrini, et al., Screening of dietary carotenoids and carotenoid-rich fruit extracts for antioxidant activities applying 2,2 '-azinobis(3-ethylenebenzothiazoline-6-sulfonic) acid radical cation decolorization assay, Oxidants Antioxid. Pt A 299 (1999) 379–389.
[18] J.H. Kim, et al., Ginsenoside F1 attenuates hyperpigmentation in B16F10 melanoma cells by inducing dendrite retraction and activating rho signalling, Exp. Dermatol. 24 (2) (2015) 150–152.
[19] T.R. Su, et al., Inhibition of Melanogenesis by Gallic acid: possible involvement of the PI3K/Akt, MEK/ERK and Wnt/beta-catenin signaling pathways in B16F10 cells, Int. J. Mol. Sci. 14 (10) (2013) 20443–20458.
[20] R. Lee, et al., Anti-melanogenic effects of extracellular vesicles derived from plant leaves and stems in mouse melanoma cells and human healthy skin, J. Extracell Vesicles 9 (1) (2020) 1703480.
[21] J.H. Kim, et al., Amino acids disrupt calcium-dependent adhesion of stratum corneum, PLoS One 14 (4) (2019), e0215244.
[22] M.L.D. Francisco, A.V.A. Resurreccion, Development of a reversed-phase high performance liquid chromatography (RP-HPLC) procedure for the simultaneous determination of phenolic compounds in peanut skin extracts, Food Chem. 117 (2) (2009) 356–363.
[23] P. Quifer-Rada, et al., A comprehensive characterisation of beer polyphenols by high resolution mass spectrometry (LC-ESI-LTQ-Orbitrap-MS), Food Chem. 169 (2015) 336–343.
[24] D.U. Jo, et al., By-product of Korean liquor fermented by Saccharomyces cerevisiae exhibits skin whitening activity, Food Sci. Biotechnol. 31 (5) (2022) 587–596.
[25] S. Chung, G.J. Lim, J.Y. Lee, Quantitative analysis of melanin content in a three-dimensional melanoma cell culture, Sci. Rep. 9 (1) (2019) 780.
[26] C.A. MacRae, R.T. Peterson, Zebrafish as tools for drug discovery, Nat. Rev. Drug Discov. 14 (10) (2015) 721–731.
[27] K. Sugimoto, et al., Inhibitory effects of alpha-arbutin on melanin synthesis in cultured human melanoma cells and a three-dimensional human skin model, Biol. Pharm. Bull. 27 (4) (2004) 510–514.
[28] S. Ikram, et al., Recovery of major phenolic acids and antioxidant activity of highland barley brewer's spent grains extracts, J. Food Process. Preserv. 44 (1) (2020).
[29] M.A. Zainal Arifin, et al., Utilization of food waste and by-products in the fabrication of active and intelligent packaging for seafood and meat products, Foods 12 (3) (2023).
[30] X.X. Peng, et al., Recycling municipal, agricultural and industrial waste into energy, fertilizers, food and construction materials, and economic feasibility: a review, Environ. Chem. Lett. 21 (2023).
[31] P. Klimek, et al., Utilizing brewer's-spent-grain in wood-based particleboard manufacturing, J. Clean. Prod. 141 (2017) 812–817.
[32] D. San Martin, et al., Brewers' spent yeast and grain protein hydrolysates as second-generation feedstuff for aquaculture feed, Waste Biomass Valoriz 11 (10) (2020) 5307–5320.
[33] T. Amoriello, et al., Technological properties and consumer acceptability of bakery products enriched with brewers' spent grains, Foods 9 (10) (2020).
[34] A.M. Ferreira, et al., Anti-melanogenic potential of natural and synthetic substances: application in zebrafish model, Molecules 28 (3) (2023).
[35] E. Camp, M. Lardelli, Tyrosinase gene expression in zebrafish embryos, Dev. Genes Evol. 211 (3) (2001) 150–153.
[36] N. Gulzar, et al., Expression of defense genes and free radical scavenging on pre supplementation of silicon to Alternaria solani inoculated Lycopersicon esculentum plants, Physiol. Mol. Plant Pathol. 123 (2023).
[37] H.C. Huang, et al., Supercritical fluid extract of Lycium chinense miller root inhibition of melanin production and its potential mechanisms of action, BMC Complement. Altern. Med. 14 (2014).
[38] C.F. Chan, et al., Fermented broth in tyrosinase- and melanogenesis inhibition, Molecules 19 (9) (2014) 13122–13135.
[39] T. Mitsunaga, K. Yamauchi, Effect of quercetin derivatives on melanogenesis stimulation of melanoma cells, J. Wood Sci. 61 (4) (2015) 351–363.
[40] E. Karg, et al., Hydrogen peroxide as an inducer of elevated tyrosinase level in melanoma cells, J. Invest. Dermatol. 100 (2 Suppl) (1993) 209S–213S.
[41] H.J. Lee, et al., Hesperidin, a popular antioxidant inhibits Melanogenesis via Erk1/2 mediated MITF degradation, Int. J. Mol. Sci. 16 (8) (2015) 18384–18395.
[42] E.S. Kim, et al., Mitochondrial dynamics regulate melanogenesis through proteasomal degradation of MITF via ROS-ERK activation, Pigment Cell Melanoma Res. 27 (6) (2014) 1051–1062.
[43] H. Ko, M.M. Kim, H2O2 promotes the aging process of melanogenesis through modulation of MITF and Nrf2, Mol. Biol. Rep. 46 (2) (2019) 2461–2471.
[44] S.K. Bardaweel, et al., Reactive oxygen species: the dual role in physiological and pathological conditions of the human body, Eurasian J. Med. 50 (3) (2018) 193–201.
[45] J.H. Kim, et al., Effect of 3,6-anhydro-l-galactose on alpha-melanocyte stimulating hormone-induced melanogenesis in human melanocytes and a skin-equivalent model, J. Cell. Biochem. 119 (9) (2018) 7643–7656.
[46] K. Maeda, M. Fukuda, Arbutin: mechanism of its depigmenting action in human melanocyte culture, J. Pharmacol. Exp. Ther. 276 (2) (1996) 765–769.
[47] J.A. Lister, Development of pigment cells in the zebrafish embryo, Microsc. Res. Tech. 58 (6) (2002) 435–441.
[48] H.J. Jeon, et al., Antimelanogenic effects of curcumin and its dimethoxy derivatives: mechanistic investigation using B16F10 melanoma cells and zebrafish (*Danio rerio*) embryos, Foods (2023) **12**(5).
[49] C.B. Kimmel, et al., Stages of embryonic development of the zebrafish, Dev. Dyn. 203 (3) (1995) 253–310.
[50] H.S. Yoon, et al., Differential effects of Methoxylated p-Coumaric Acids on melanoma in B16/F10 cells, Prev. Nutr. Food Sci. 20 (1) (2015) 73–77.